Rapid Communications

# Dynamic heterogeneity and conditional statistics of non-Gaussian temperature fluctuations in turbulent thermal convection

Xiaozhou He,[1,*] Yin Wang,[2] and Penger Tong[2]

[1]*School of Mechanical Engineering and Automation, Harbin Institute of Technology, 518055 Shenzhen, China*

[2]*Department of Physics, Hong Kong University of Science and Technology, Clear Water Bay, Kowloon, Hong Kong*

(Received 22 December 2017; published 14 May 2018)

Non-Gaussian fluctuations with an exponential tail in their probability density function (PDF) are often observed in nonequilibrium steady states (NESSs) and one does not understand why they appear so often. Turbulent Rayleigh-Bénard convection (RBC) is an example of such a NESS, in which the measured PDF $P(\delta T)$ of temperature fluctuations $\delta T$ in the central region of the flow has a long exponential tail. Here we show that because of the dynamic heterogeneity in RBC, the exponential PDF is generated by a convolution of a set of dynamics modes conditioned on a constant local thermal dissipation rate $\epsilon$. The conditional PDF $G(\delta T|\epsilon)$ of $\delta T$ under a constant $\epsilon$ is found to be of Gaussian form and its variance $\sigma_T^2$ for different values of $\epsilon$ follows an exponential distribution. The convolution of the two distribution functions gives rise to the exponential PDF $P(\delta T)$. This work thus provides a physical mechanism of the observed exponential distribution of $\delta T$ in RBC and also sheds light on the origin of non-Gaussian fluctuations in other NESSs.

DOI: 10.1103/PhysRevFluids.3.052401

While much is known about fluctuations at equilibrium, our current understanding of fluctuations in nonequilibrium states is rather limited [1]. Because most equilibrium processes, such as Brownian motion of molecules, usually have a finite correlation time, their fluctuations will eventually be randomized after a sufficiently long delay time, to which the central limit theorem applies and thus they follow the Gaussian statistics. Nonequilibrium states, on the other hand, differ significantly from the equilibrium ones in that they often involve a net flux of mass, momentum, or heat with a long correlation time, so that they do not follow the Gaussian statistics. Experimentally, a nonequilibrium state can be generated by applying a generalized force, such as a gradient of concentration, temperature, velocity, or (chemical) potential, to the system. When the generalized force is a constant independent of time, the system can be driven into a nonequilibrium steady state (NESS), which is perhaps the simplest class of nonequilibrium states [2,3].

Turbulent Rayleigh-Bénard convection (RBC) is an example of such a NESS, in which a confined fluid layer of thickness $H$ is heated from below and cooled from the top with a constant vertical temperature gradient parallel to gravity. When the temperature difference $\Delta T$ across the fluid layer or its dimensionless expression, the Rayleigh number Ra [4], is sufficiently large, the bulk fluid becomes turbulent and heat is transported predominantly by convection. In the past decades, considerable experimental and theoretical efforts have been made to understand the observed scaling laws in turbulent heat transport and temperature and velocity fluctuations over varying Rayleigh numbers [5–9]. An intriguing feature of RBC is the continuing appearance of large fluctuations in the temperature field, which do not follow the Gaussian statistics [10]. As shown in Fig. 1 below, the measured probability density function (PDF) $P(\delta T)$ of temperature fluctuations $\delta T$ from the

*Corresponding author: hexiaozhou@hit.edu.cn

 

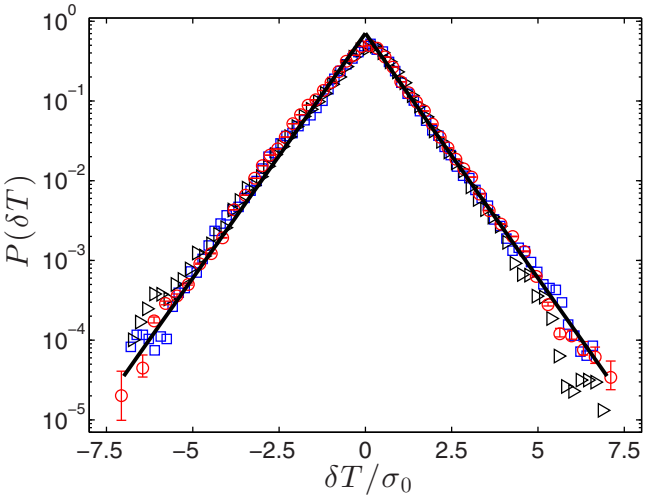


FIG. 1. Measured unconditional PDF $P(\delta T)$ of temperature fluctuations $\delta T$ at the cell center for three different values of Ra: $1.3 \times 10^9$ (blue squares), $3.8 \times 10^9$ (black triangles), and $8.3 \times 10^9$ (red circles). In the plot, $\delta T$ is normalized by its rms value $\sigma_0$, and the error bars show the standard deviation of the red circles. The solid line shows a plot of Eq. (4).

mean value in the central region of the cell has a long exponential tail with its amplitude varied by more than 4 decades, which falls off much slower than a Gaussian. The exponential PDF was found in a wide dynamic range with Ra varied from $4 \times 10^7$ up to $10^{15}$, and its functional form remains universal and independent of Ra, once $\delta T$ is normalized by its standard deviation $\sigma_0$ [5,11–14]. It was observed in various convecting fluids, such as low-temperature helium gas [5,11,14], mercury [12], sulfur hexafluoride gas [15], fluorocarbon FC72 [16], and water [13,17,18]. These measurements have stimulated considerable theoretical efforts [5,8,19–21], aimed at explaining the dynamic origin of the anomalously large temperature fluctuations. While the physical mechanism of the non-Gaussian behavior in RBC still remains elusive, it was believed that the large temperature fluctuations are probably produced by the thermal plumes, which are intermittently emitted from the thermal boundary layers (BLs) and carry temperature fluctuations from the BLs to the bulk region of the flow [10,19].

Intriguingly, non-Gaussian fluctuations were also observed in other turbulent flows, such as turbulent jet, grid-generated turbulence and counterrotating flows [19,20,22–24], and in other nonequilibrium processes ranging from granular gas and plasma [25–28] to the dynamics of active matter and protein motion in living cells [29,30]. Given the large variety of nonequilibrium systems involved, it is unlikely that all of the non-Gaussian fluctuations are produced by a single mechanism. A number of theoretical models have been proposed to explain the non-Gaussian behavior in the flow systems [19,21,22,24,31]. Different approximations and assumptions were made in order to fit the experimental data [8,31]. An interesting hypothesis states that because of the dynamic heterogeneity in the system, non-Gaussian fluctuations can be generated by a convolution of Gaussian-like dynamic modes, to which the central limit theorem applies. In this case, one can write [19,24,29–32]

$$P(\delta T) = \int_0^\infty G(\delta T|\epsilon) f(\epsilon) d\epsilon, \tag{1}$$

where the conditional PDF $G(\delta T|\epsilon)$ has a Gaussian form

$$G(\delta T|\epsilon) = \frac{1}{\sqrt{2\pi}\sigma_T(\epsilon)} e^{-\delta T^2/[2\sigma_T^2(\epsilon)]}, \tag{2}$$

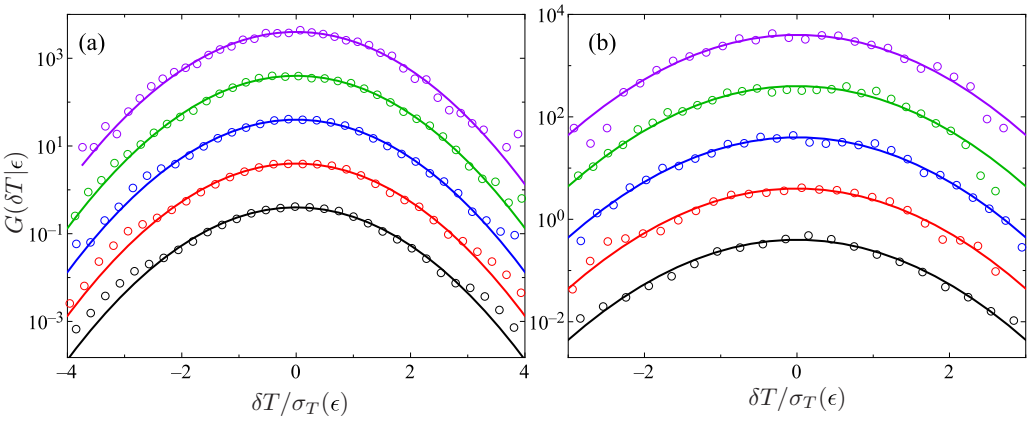


FIG. 2. (a) Measured conditional PDF $G(\delta T|\epsilon)$ for five different values of $\epsilon$ in units of their rms value $\sigma_\epsilon$ (from bottom to top): $\epsilon/\sigma_\epsilon = 0.2$ (black circles), 0.5 (red circles), 2 (blue circles), 5 (green circles), and 10 (purple circles). The measurements were made at the cell center with $\mathrm{Ra} = 8.3 \times 10^9$. In the plot, $\delta T$ is conditioned at a fixed value of $\epsilon$ and is normalized by the corresponding rms value $\sigma_T(\epsilon)$. For clarity, the vertical scale of the four PDFs with $\epsilon/\sigma_\epsilon \geqslant 0.5$ is multiplied by a factor 10, $10^2$, $10^3$, and $10^4$, respectively. The solid lines represent Gaussian functions expressed by Eq. (2) with different variance $\sigma_T^2(\epsilon)$. (b) Similar plot of $G(\delta T|\epsilon)$ obtained at the cell center with $\mathrm{Ra} = 1.8 \times 10^9$. The data sets are obtained at five different values of $\epsilon$ in units of their rms value $\sigma_\epsilon$ (from bottom to top): $\epsilon/\sigma_\epsilon = 2$ (black), 4 (red), 6 (blue), 8 (green), and 10 (purple). For clarity, the vertical scale of the four PDFs with $\epsilon/\sigma_\epsilon \geqslant 4$ is multiplied by a factor 4, $4^2$, $4^3$, and $4^4$, respectively. The solid lines show the Gaussian fits of Eq. (2) to the data points with different values of $\sigma_T(\epsilon)$.

when the dynamic variable $\epsilon$ is held constant. Here the variance $\sigma_T^2(\epsilon)$ is a function of $\epsilon$. For a given nonequilibrium system, the challenge is to identify the correct dynamic variable $\epsilon$ and its PDF $f(\epsilon)$.

In this Rapid Communication, we show with solid experimental evidence that non-Gaussian temperature fluctuations in RBC are generated by the thermal plumes detached from the thermal boundary layers, which can be uniquely characterized by the local thermal dissipation rate $\epsilon(t) \equiv \kappa[\nabla T(t)]^2$. With this correct dynamic variable, the exponential PDF $P(\delta T)$ is explained by the measured dynamic heterogeneity of the local thermal dissipation rate owing to rapid mixing and advection of warm and cold plumes passing through the central region of the cell. It is found (see Figs. 2 and 6 below) that the conditional PDF $G(\delta T|\epsilon)$ of the temperature time series data $\delta T(t)$ indeed follows the Gaussian statistics and its variance $\sigma_T^2(\epsilon)$ has an exponential-like distribution

$$F\left(\sigma_T^2\right) = f(\epsilon)\frac{d\epsilon}{d\sigma_T^2(\epsilon)} = \frac{1}{\sigma_0^2}e^{-\sigma_T^2/\sigma_0^2}, \tag{3}$$

where $\sigma_0^2$ is the mean value of $\sigma_T^2(\epsilon)$ and $f(\epsilon)$ is the PDF obtained from the time series data $\epsilon(t)$, which is simultaneously measured together with $\delta T(t)$. With Eqs. (1)–(3), we find the unconditional PDF

$$P(\delta T) = \frac{1}{\sqrt{2}\sigma_0}e^{-\sqrt{2}|\delta T/\sigma_0|}. \tag{4}$$

Equation (4) thus provides a physical explanation of the observed exponential form of $P(\delta T)$ in RBC.

The convection experiment was conducted in an upright cylinder with the inner diameter $D = 19.0$ cm and height $H = 20.5$ cm, and thus the corresponding aspect ratio $\Gamma \equiv D/H = 0.93$. The entire convection cell was placed inside a thermostat box, whose temperature was set to $30 \pm 0.3\,^\circ$C, which matches the temperature of the bulk fluid (deionized water). In the experiment, the value of Ra was varied in the range $10^9 \lesssim \mathrm{Ra} \lesssim 10^{10}$ and the Prandtl number Pr was fixed at $\mathrm{Pr} \simeq 5.4$.

Measurements of the local thermal dissipation rate $\epsilon(t)$ at the cell center were made using a homemade temperature gradient probe, which consists of four identical thermistor beads 127 $\mu$m in diameter and 15 ms in time constant. One of the thermistors was placed at the origin (labeled as $T_0$), and the other three (labeled as $T_i$) were placed along the $i = x$, $y$, and $z$ axes, respectively. By simultaneously measuring the four temperature signals, we obtained the three temperature gradient components $\Delta T_i/\Delta\ell$, where $\Delta T_i = T_i - T_0$ is the temperature difference between a pair of the thermistors with separation $\Delta\ell = 250 \pm 100$ $\mu$m. This gradient probe has an adequate spatial resolution to resolve the thermal boundary-layer thickness $\lambda$ ($\simeq$0.8 mm at Ra $\simeq 3.6 \times 10^9$), which is the smallest length scale in RBC. All the thermistors were calibrated individually with an accuracy of 5 mK for each $\Delta T_i$. The sampling rate of the temperature measurements was set at 40 Hz. Typically, we took 7-h-long time series ($\sim 10^6$ data points) at each value of Ra, ensuring that the statistical average is adequate. Other details about the apparatus and experimental method can be found in [18,33].

Figure 1 shows the measured unconditional PDF $P(\delta T)$ at the cell center for three different values of Ra. The local temperature signals were obtained from a single thermistor. Although the measured rms value $\sigma_0$ varies considerably for different Ra, the PDFs collapse onto a single master curve, once the normalized variable $\delta T/\sigma_0$ is used. Except for a small roundoff near the origin, all of the PDFs have an exponential tail (solid line). Figure 1 thus reveals that $P(\delta T)$ has a universal form independent of Ra. As mentioned above, such an exponential PDF was also observed in the previous convection experiments. Evidently, the exponential PDF is a leptokurtic distribution, which has a higher peak and a heavier tail compared with the Gaussian PDF [34].

To obtain the conditional PDF $G(\delta T|\epsilon)$, one needs to select a subset of temperature fluctuations $\delta T(t_i)$ at a given value $\epsilon_i$ of the local thermal dissipation rate. This is achieved by first finding all the time stamps $t_i$, at which the measured values of $\epsilon(t_i)$ fall within $\epsilon_i + \delta\epsilon$, where $\delta\epsilon$ is a predetermined bin width. The subset of $\delta T(t_i)$ is then selected from the temperature time series data, which are simultaneously measured with the same time stamps $t_i$. Figure 2(a) shows a representative set of the conditional PDFs $G(\delta T|\epsilon)$ for five different values of $\epsilon$, which are obtained at the cell center with Ra $= 8.3 \times 10^9$. It is seen that all of the conditional PDFs can be well described by a Gaussian function given in Eq. (2) with $\sigma_T^2(\epsilon)$ being the variance of the conditionally sampled $\delta T(t_i)$. Similarly, the conditional PDFs obtained at other values of Ra are found to have the same Gaussian form, as shown in Fig. 2(b).

Figure 3 shows how the obtained values of $\sigma_T^2(\epsilon)/\sigma_0^2$ change with $\epsilon/\sigma_\epsilon$. The data can be well described by the power law

$$\frac{\sigma_T^2(\epsilon)}{\sigma_0^2} = a\left[\frac{\epsilon}{\sigma_\epsilon}\right]^\alpha, \tag{5}$$

with $a = 2.853$ and $\alpha = 0.363$ (solid line). The bin size $\delta\epsilon$ used in Fig. 3 does not change the Gaussian form of the obtained $G(\delta T|\epsilon)$ nor the power-law dependence of $\sigma_T^2(\epsilon)/\sigma_0^2$ as shown in Eq. (5). [(It only changes the error bar of the resulting $\sigma_T^2(\epsilon)$.] From the temperature resolution of 5 mK, we determine the minimal value $\epsilon_{\min}$ that our gradient probe can resolve. For Ra $= 8.3 \times 10^9$, we find the normalized resolution of $\epsilon$ is $\epsilon_{\min}/\sigma_\epsilon \simeq 0.043$, which is the lowest value of $\epsilon/\sigma_\epsilon$ shown in Fig. 3.

To understand why the conditionally sampled $\delta T$ at a constant $\epsilon$ has a Gaussian form, we examined the temperature PDFs near the lower conducting plate. As a wall-bounded flow, RBC has a temperature BL adjacent to each conducting plate and its thickness $\delta$ decreases with increasing Ra. Because most of the temperature difference $\Delta T$ across the cell drops within the two BLs, the local dissipation profile $\epsilon(z)$ across the lower (or upper) BL is predominantly determined by the large mean temperature gradient and is a unique function of distance $z$ (or $H - z$) away from the conducting plate [33,35,36]. As a result, temperature fluctuations at a fixed position $z$ are equivalently conditioned at a constant $\epsilon$. Figure 4 shows the measured $P(\delta T)$ at two constant values of $z/\delta = 0.14$ and $z/\delta = 0.46$. Indeed, the measured PDFs have a Gaussian form, which is consistent with the results shown in Fig. 2.

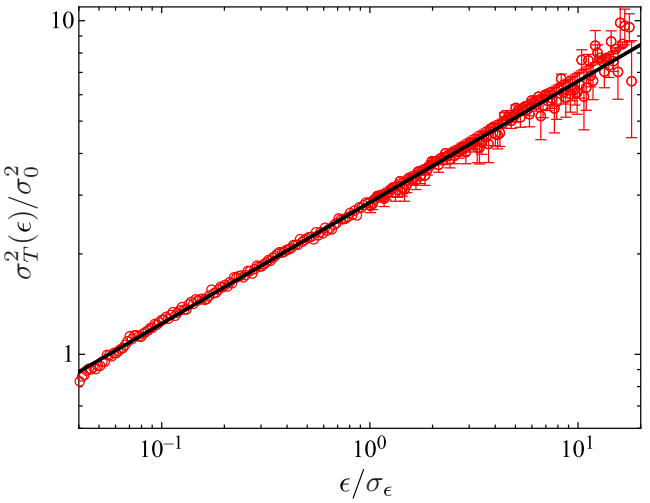


FIG. 3. Obtained values of $\sigma_T^2(\epsilon)/\sigma_0^2$ as a function of $\epsilon/\sigma_\epsilon$ (red circles). The measurements were made at the cell center with Ra $= 8.3 \times 10^9$. The error bars indicate the bin size $\delta\epsilon$ used to digitize the measured $\epsilon$. The solid line shows a power-law fit of Eq. (5) with $a = 2.853$ and $\alpha = 0.363$ to the data points for $\epsilon/\sigma_\epsilon > 0.043$.

In a recent work [36], we found that the measured mean temperature boundary-layer profile agrees well with the direct numerical simulation results, suggesting that the small thermistor has a negligible effect on the measurement. We believe that the main effect of the thermistor size is to introduce a (spatial) running average over the measured profile, which only averages out small-scale fluctuations (comparable to the thermistor size) but does not affect the functional form of the smooth mean temperature profile. As for the temporal response of the thermistor used in the experiment, its time constant is smaller than 15 ms, which is fast enough to resolve the entire temperature power spectrum [33].

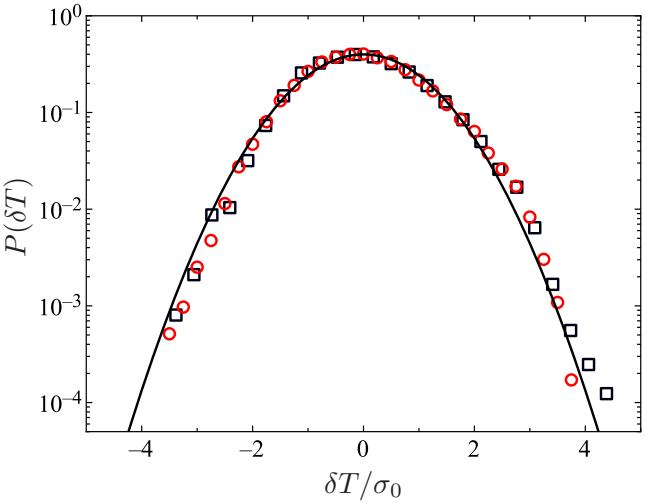


FIG. 4. Measured unconditional PDF $P(\delta T)$ of temperature fluctuations $\delta T$ in the boundary-layer region with $z/\delta = 0.14$ (black squares) and $z/\delta = 0.46$ (red circles). The measurements were made in the $\Gamma = 1$ upright cylinder with fixed values of Ra $= 6.8 \times 10^9$ and Pr $= 4.4$ (water). In the plot, $\delta T$ is normalized by its rms value $\sigma_0$. The solid line shows a plot of the standard Gaussian function.

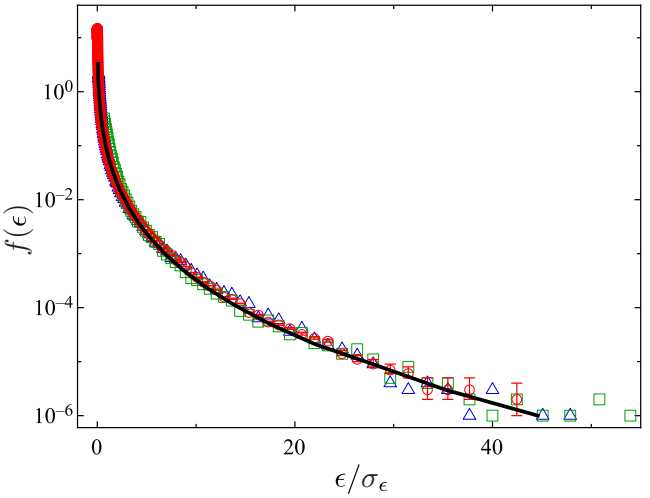


FIG. 5. Measured PDF $f(\epsilon)$ of the local thermal dissipation rate $\epsilon$ at the cell center for three different values of Ra: $1.3 \times 10^9$ (green squares), $3.8 \times 10^9$ (blue triangles), and $8.3 \times 10^9$ (red circles). In the plot, $\epsilon$ is normalized by its rms value $\sigma_\epsilon$, and the error bars show the standard deviation of the circles. The solid line is a plot of Eq. (6) with $a = 2.853$ and $\alpha = 0.363$.

As the thermal plumes at the cell center are detached from the temperature BLs, their statistics is expected to be similar to that inside the temperature BLs. However, because of the random advection of thermal plumes across the measuring position, the unconditional PDF $P(\delta T)$ samples temperature fluctuations with a variety of temperature variance $\sigma_T^2(z)$ [or $\sigma_T^2(\epsilon)$]. The conditional PDF $G(\delta T|\epsilon)$, on the other hand, filters out the dynamic heterogeneity and only samples those temperature fluctuations with a fixed value of $\epsilon$ [or $\sigma_T^2(\epsilon)$], so that it has the same Gaussian form as that measured at a fixed position $z$ inside the temperature BL. Because of strong turbulent mixing at the cell center, the distribution of $\sigma_T^2(\epsilon)$ is expected to be broad.

Figure 5 shows the measured PDF $f(\epsilon)$ at the cell center for three different values of Ra. The PDFs obtained at different Ra can all be brought into coincidence, once $\epsilon$ is normalized by its rms value $\sigma_\epsilon$. Plots of $f(\epsilon)$ vs $\epsilon/\sigma_\epsilon$ remain unchanged in the Ra range studied and only $\sigma_\epsilon$ changes with Ra. With the measured $f(\epsilon)$ and calculated $d\epsilon/d\sigma_T^2$ from the fitting result shown in Eq. (5), we numerically obtain $F(\sigma_T^2)$ by using Eq. (3), which is shown in Fig. 6. The obtained $F(\sigma_T^2)$ (red circles) indeed has a broad distribution and can be well described by a simple exponential function given in Eq. (3) (solid line).

Figures 2–6 thus confirm Eqs. (1)–(3), which lead to the final exponential form of the unconditional PDF $P(\delta T)$, as shown in Eq. (4). The solid line in Fig. 1 shows a plot of Eq. (4) without any additional fitting parameter, which describes the data very well. The above results thus demonstrate that the proposed decomposition of non-Gaussian temperature fluctuations into a set of Gaussian-like dynamic modes conditioned on a constant local thermal dissipation rate $\epsilon$ works.

Furthermore, with the exponential PDF $F(\sigma_T^2)$, one can derive the functional form of $f(\epsilon)$ using Eq. (3) as

$$f(\epsilon) = \frac{a\alpha}{\sigma_\epsilon}(\epsilon/\sigma_\epsilon)^{\alpha-1} e^{-a(\epsilon/\sigma_\epsilon)^\alpha}, \tag{6}$$

where $a$ and $\alpha$ are given in Eq. (5). The solid line in Fig. 5 shows a plot of Eq. (6) without any additional fitting parameter, which describes the data very well. This result further confirms that the data shown in Figs. 2–6 are consistent with each other, and the consistency remains the same for all the values of Ra in the range studied. A similar stretched $\Gamma$-function form for $f(\epsilon)$ was derived [37]

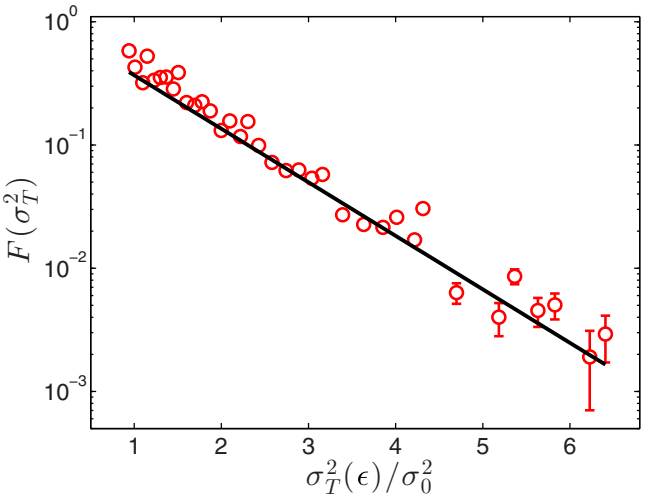


FIG. 6. Numerically obtained PDF $F(\sigma_T^2)$ of temperature variance $\sigma_T^2$ for $\mathrm{Ra} = 8.3 \times 10^9$ at the cell center. The error bars show the standard deviation of the data points. The solid line is a plot of Eq. (3).

in a previous theoretical study of intermittent dissipation of a passive scalar in turbulence when the Péclet number $\mathrm{Pe} \to \infty$.

## ACKNOWLEDGMENTS

We thank P.-Y. Lai and Bruce J. Ackerson for useful discussions. X.H. was supported by the China Thousand Young Talents Program and the National Natural Science Foundation of China under Grant No. 11772111. P.T. was supported by the Hong Kong Research Grants Council under Grants No. C6004-14G and No. A-HKUST616/14-A.

[1] D. Ruelle, Conversations on nonequilibrium physics with an extraterrestrial, Phys. Today **57**(5), 48 (2004).
[2] R. Zia and B. Schmittmann, A possible classification of nonequilibrium steady states, J. Phys. A: Math. Gen. **39**, L407 (2006).
[3] T. Speck, V. Blickle, C. Bechinger, and U. Seifert, Distribution of entropy production for a colloidal particle in a nonequilibrium steady state, Europhys. Lett. **79**, 30002 (2007).
[4] The Rayleigh number Ra is defined as $\mathrm{Ra} \equiv \alpha g \Delta T H^3/\nu\kappa$, where $g$ is the gravitational acceleration, $\Delta T$ is the temperature difference across the fluid layer of thickness $H$, and $\alpha$, $\nu$, and $\kappa$ are, respectively, the thermal expansion coefficient, and the viscous and thermal diffusivity of the convecting fluid. The Prandtl number Pr is defined as $\mathrm{Pr} \equiv \nu/\kappa$.
[5] B. Castaing, G. Gunaratne, F. Heslot, L. Kadanoff, A. Libchaber, S. Thomae, X. Z. Wu, S. Zaleski, and G. Zanetti, Scaling of hard thermal turbulence in Rayleigh-Bénard convection, J. Fluid Mech. **204**, 1 (1989).
[6] E. D. Siggia, High Rayleigh number convection, Annu. Rev. Fluid Mech. **26**, 137 (1994).
[7] G. Ahlers, S. Grossmann, and D. Lohse, Heat transfer and large scale dynamics in turbulent Rayleigh-Bénard convection, Rev. Mod. Phys. **81**, 503 (2009).
[8] D. Lohse and K.-Q. Xia, Small-scale properties of turbulent Rayleigh-Bénard convection, Annu. Rev. Fluid Mech. **42**, 335 (2010).
[9] F. Chillà and J. Schumacher, New perspectives in turbulent Rayleigh-Bénard convection, Eur. Phys. J. E **35**, 58 (2012).
[10] L. P. Kadanoff, Turbulent heat flow: Structures and scaling, Phys. Today **54**(8), 34 (2001).
[11] M. Sano, X. Z. Wu, and A. Libchaber, Turbulence in helium-gas free convection, Phys. Rev. A **40**, 6421 (1989).

[12] J. P. Gollub, J. Clarke, M. Gharib, B. Lane, and O. N. Mesquita, Fluctuations and Transport in a Stirred Fluid with a Mean Gradient, Phys. Rev. Lett. **67**, 3507 (1991).
[13] Y.-B. Du and P. Tong, Temperature fluctuations in a convection cell with rough upper and lower surfaces, Phys. Rev. E **63**, 046303 (2001).
[14] J. J. Niemela, L. Skrbek, K. R. Sreenivasan, and R. J. Donnelly, Turbulent convection at very high Rayleigh numbers, Nature (London) **404**, 837 (2000).
[15] A. Belmonte, A. Tilgner, and A. Libchaber, Temperature and velocity boundary layers in turbulent convection, Phys. Rev. E **50**, 269 (1994).
[16] P. Wei and G. Ahlers, On the nature of fluctuations in turbulent Rayleigh-Bénard convection at large Prandtl numbers, J. Fluid Mech. **802**, 203 (2016).
[17] S. Q. Zhou and K.-Q. Xia, Plume Statistics in Thermal Turbulence: Mixing of An Active Scalar, Phys. Rev. Lett. **89**, 184502 (2002).
[18] X. He, P. Tong, and K.-Q. Xia, Measured Thermal Dissipation Field in Turbulent Rayleigh-Bénard Convection, Phys. Rev. Lett. **98**, 144501 (2007).
[19] B. I. Shraiman and E. D. Siggia, Lagrangian path integrals and fluctuations in random flow, Phys. Rev. E **49**, 2912 (1994).
[20] A. Pumir, B. Shraiman, and E. D. Siggia, Exponential Tails and Random Advection, Phys. Rev. Lett. **66**, 2984 (1991).
[21] E. S. C. Ching, Probability Densities of Turbulent Temperature Fluctuations, Phys. Rev. Lett. **70**, 283 (1993).
[22] B. Shraiman and E. D. Siggia, Scalar turbulence, Nature (London) **405**, 639 (2000).
[23] Jayesh and Z. Warhaft, Probability Distribution of A Passive Scalar in Grid-Generated Turbulence, Phys. Rev. Lett. **67**, 3503 (1991).
[24] L. Chevillard, S. G. Roux, E. Levêque, N. Mordant, J.-F. Pinton, and A. Arneodo, Lagrangian Velocity Statistics in Turbulent Flows, Phys. Rev. Lett. **91**, 214502 (2003).
[25] W. Chen and K. To, Unusual diffusion in a quasi-two-dimensional granular gas, Phys. Rev. E **80**, 061305 (2009).
[26] J. S. Van Zon and F. C. MacKintosh, Velocity Distributions in Dissipative Granular Gases, Phys. Rev. Lett. **93**, 038001 (2004).
[27] F. Rouyer and N. Menon, Velocity Fluctuations in A Homogeneous 2D Granular Gas in Steady State, Phys. Rev. Lett. **85**, 3676 (2000).
[28] B. Liu and J. Goree, Superdiffusion and Non-Gaussian Statistics in a Driven-Dissipative 2D Dusty Plasma, Phys. Rev. Lett. **100**, 055003 (2008).
[29] B. Wang, J. Kuo, S. C. Bae, and S. Granick, When Brownian diffusion is not Gaussian, Nat. Mater. **11**, 481 (2012).
[30] W. He, H. Song, Y. Su, L. Geng, B. J. Ackerson, H. B. Peng, and P. Tong, Dynamic heterogeneity and non-Gaussian statistics for acetylcholine receptors on live cell membrane, Nat. Commun. **7**, 11701 (2016).
[31] A. K. Aringazin and M. I. Mazhitov, One-dimensional Langevin models of fluid particle acceleration in developed turbulence, Phys. Rev. E **69**, 026305 (2004).
[32] A. Naert, B. Castaing, B. Chabaud, B. Hébral, and J. Peinke, Conditional statistics of velocity fluctuations in turbulence, Physica D **113**, 73 (1998).
[33] X. He and P. Tong, Measurements of the thermal dissipation field in turbulent Rayleigh-Bénard convection, Phys. Rev. E **79**, 026306 (2009).
[34] C. Walck, Handbook on statistical distributions for experimentalists. Internal Report SUFPFY/9601 (University of Stockholm, 2007).
[35] Y. Wang, X. He, and P. Tong, Boundary layer fluctuations and their effects on mean and variance temperature profiles in turbulent Rayleigh-Bénard convection, Phys. Rev. Fluids **1**, 082301(R) (2016).
[36] Y. Wang, W. Xu, X. He, H.-F. Yik, X.-P. Wang, J. Schumacher, and P. Tong, Boundary layer fluctuations in turbulent Rayleigh-Bénard convection, J. Fluid Mech. **840**, 408 (2018).
[37] M. Chertkov, G. Falkovich, and I. Kolokolov, Intermittent Dissipation of a Passive Scalar in Turbulence, Phys. Rev. Lett. **80**, 2121 (1998).